

Dear Friederike Wagner-Cremer,

Please see our reply according to the comments of the referees below:

Referee # 1 Bückner, Christian

This is a really well written paper including a very careful treatment and analysis of downhole data. However, the relation between gamma ray and deltaO18 is not a perfect one ($R^2 = 0,6$), and I would like to have discussed this fact a bit more. What is the causal effect for the relation, and why is there no better relation?

Reply:

Thank you for your comment. We have tried other fits (e.g. exponential) as well and best results were gained by the linear relationship. We agree, that the R^2 of 0,6 for the linear solution is rather low. It suggests that the relationship between the synthetic deltaO18 (calculated from gamma ray) and the original data set (deltaO18) is not completely linear.

We suggest the following reasons of the GR signature:

1) Climate dependent supply and deposition of K-rich clastics (feldspars, clays). They are increased during cold-dry periods (high GR) and decreased during warm-wet periods (high carbonate deposition; low GR) in the sediments.

2) Tephra layers that are partly recognizable in the GR / K data (increased GR). Even if the prominent layers at 20 and 68 mblf could be removed, at least 6 additional tephra layers (see tephra pointers; Fig. 2b) were identified in the cores down to 240 mblf. These thin layers (thickness < 10 cm) are not recognizable easily in the GR data and could not be removed but are assumed to contribute to the GR / K curve. Their occurrence in zones A and C (Fig. 2c; zones of decreased synthetic deltaO18) suggest that they have an effect on the GR signature.

3) Variations in the catchment area. Outcrops of Triassic carbonates and clastics occur in large parts in Lake Ohrid's catchment area. Furthermore, ophiolites, magmatic and metamorphic rocks are exposed and are potential sources of terrestrial material. Erosion and transport of these rocks, e.g. by means of surface runoff into the lake, was likely variable over time and subsequently the input of K-bearing particles.

Therefore, the GR is most likely controlled by several factors and cannot be described in total by linear solution. However, the main component seems to be a linear response of K-rich sediments to the global climate trend (1). Further, we consider the attempt useful to compare both datasets and to show the very unusual similarity in cyclic characteristic between LR04 and GR.

If you agree, we will add this part to the discussion section.

Changes according to comments from referee # 1:

Page 12, line 11-20 (p. 7684, line 8-18): We have deleted “Under the assumption ... deposition of clastics.” and have inserted the reply “We suggest the ... between LR04 and GR.” because we agree that the GR signature should be further clarified.

Referee # 2 Anonymous referee

1. I think your correlations are correct and straightforward and because the LR04 record is astronomically tuned this provides a solid age model on its own for Lake Ohrid. I do not understand why you bring in the tephrostratigraphy component. These tephra layers do come from outside Lake Ohrid and as such bring in extra potential correlation errors. I do not see why this is useful and believe it makes your story weaker.
2. Additional comments: Please use ka (1000 years) and Ma (million years) for ages and kyr (1000 years) and Myr (million years) for duration. Change throughout the text. So give sed. rates in cm/kyr.
3. The title should read: Age-depth model (instead of Age depth-model) for the past 630 kyr. And I would also not use the term Macedonia for the FYROM as this may upset some other communities in the area.
4. Abstract: please write “can thus/only/potentially be” instead of “can be thus” (page 1 line 21; page 3 line 17 and line 22)
5. Do you have an explanation why the sed. rates shift exactly at 110 mblf?
6. Suggestions: Page 3 line 20: use another word for “trigger” (e.g. reflect)
7. Page 5 line 1-2: Give references and explain in more detail what age control is already present.
8. Page 6 line 23-27: “in conjunction with age control points from tephra layers” ... They need to be identified in the core by visual description or by physical properties”. I think this is a bit misleading paragraph as it suggests you present ages from tephras of their Lake Ohrid core, which is not the case!
9. Page 7 lines 21-25: Why do you describe all this if at the end you tell us it could not be used? Suggest to delete the part from “Therefore ...However,” and start again with “Porosity ...
10. Page 8 lines 9-12: It is unclear to me why and how the eight age depth-points have been brought into the Lake Ohrid record. I do not see the added value here. Moreover, the reliability of all these references are not discussed. For instance how solid are all these ages, how reliable is their correlation, etc. Why do you need these “anchor points”?
11. Page 9 equations??? Why do this? This is elementary school maths!

12. Page 12 line 4- 5: "Further interpretation was postponed" reads as you want to slice the results into another paper. Suggest delete or give some interpretations.

Reply:

1. (10.) We agree that the LR04 record is astronomically tuned and widely used to construct age models for marine as well as for lacustrine sediment archives. Nevertheless, the use of reference records for orbital tuning contains some general obstacles. The cyclic “saw tooth” pattern of LR04 involve the risk of mismatching of a certain cycle due to its repeating shape; in the section of interest it could easily lead to an correlation error of 100 kyr. Even if the correlation in between our data and LR04 seems extraordinary high and leaves little space for false correlation, we consider it to be of high importance to add independent age depth points from tephrochronology to limit the temporal range and secure the visual correlation. These points have uncertainties of max. 6 ka and are identified in the cores by chemical fingerprinting. According to Leicher et al. (2015), all of the eight layers which are used in this work, were macroscopically identified in the cores. By use of total alkali silica diagrams (Le Bas et al., 1992), all of the layers were unambiguously correlated to Italian volcanoes. The correlation was cross-evaluated with the occurrence of these tephra layers in other, proximal archives (Leicher et al., 2015). The absolute ages of the correlated tephra layers and their reliability are assessed in detail by Leicher et al. (2015). Furthermore, the results from tephrostratigraphy show a very good agreement with the correlation to LR04. There from we consider the tephra layers as integral component of the presented age-depth model and do not agree that they weaken our story.
2. We have changed sedimentation rates from cm/ka into cm/kyr in accordance with the referee.
3. We have changed Macedonia into FYROM and have replaced “age depth-model” by “age-depth model” throughout the complete manuscript, as suggested.
4. We have deleted “These variations in gamma ray and potassium values strongly correlate with fluctuations in global $\delta^{18}\text{O}$ values and can be thus considered a reliable proxy to depict glacial-interglacial cycles, with high clastic input during cold and / or drier periods and high carbonate precipitation during the warm and / or humid periods in Lake Ohrid.” And have inserted: “Gamma ray (GR) fluctuations and potassium (K) values from downhole logging data obtained in the sediments of Lake Ohrid from 0 to 240 mblf correlate with fluctuations in $\delta^{18}\text{O}$ values from the global benthic isotope stack LR04 (Lisiecki and Raymo, 2005). GR and K values are considered a reliable proxy to depict glacial-interglacial cycles, with high clastic input during cold and / or drier periods and high carbonate precipitation during warm and / or humid periods at Lake Ohrid.”
5. In our opinion such rapid change of the sedimentation rates at a depth of 110 mblf is rather unlikely. We assume the shift of the sedimentation rates to be an artificial feature of the sliding window analysis and consider the more variable nature of the sedimentation rates from tying to LR04 to be more realistic (Fig. 4). Based on our results we interpret glacial vs. interglacial conditions to have had an effect on sediment accumulation with increased

sedimentation rates during periods of high input of siliciclastics-rich sediments and decreased sedimentation rates during interglacial periods.

6. Page 3 line 20 (p. 7674, line 12): We have deleted “can trigger cyclic changes in the logging data” and have inserted “can be reflected by cyclic changes in the logging data”.
7. Page 5 line 1-2 (p. 7678, lines 1-2): The age control is provided by tephra layers; those individual eight layers are referenced in table 1 and details are discussed in Leicher et al. (2015). Further age control is provided by cross-checking of the age model from cores, given in Francke et al. (2015).
8. Page 6 line 23-27 (p. 7678, line 1-6): We think that it is clearly stated, that no physical ages of dating of the tephra layers are presented and that we have used stratigraphically aligned tephra layers in the cores to achieve age control points (Leicher et al., 2015). In order to emphasize this point, we have changed “in conjunction with age control points from tephra layers” into “in conjunction with stratigraphically aligned tephra layers in the cores”.
9. Page 7 lines 21-25 (p. 7679, lines 7-12): We agree and have deleted the lines as proposed by the referee.
11. Page 9, Eq. (3), (4): We agree that these equations are simple but we do not see that they lower the quality of our work.
12. Page 12, line 4-5 (p. 7684, lines 26-28): We agree that the outlook on future planned publications should not be part of this work. There from we have deleted the lines as suggested.

Further modifications

In addition to the aforementioned changes, we propose some more minor changes in the article, which are also indicated in the track change version. Furthermore, we would like to include the following aspects that evolved during revising of the article, because we are convinced that they complement our work.

- | | |
|---|---|
| Page 2, line 26-29
p. 7673, line 2-5 | We have shifted the lines to line 21-23 to keep the chronological order of pre-site studies and the ICDP drilling campaign. |
| Page 4, 25-27
p. 7675, line 12-14 | We have restructured this part and moved the section to page 4, lines 13-15. |
| Page 5, line 10
p. 7675, line 27 | We have inserted “last glacial cycle” to clarify that pre-studies were focused on this time range. |
| Page 5, line 15
p. 7676, line 3 | We have inserted “parallel and overlapping” because this important aspect might not be obvious for readers. |

Page 6, lines 28-29 p. 7677, line 23-24	We have deleted the sentence because it repeats information that is given on the previous page.
Page 7, line 27 p. 7679, line 2	We have modified Eq. 1 by using the correct symbol for porosity (Φ) and have changed this throughout the manuscript.
Page 9, line 1 p. 7680, line 14	We have replaced “age scale” by “time scale” throughout the article.
Page 10, line 16 p. 7682, line 5	We have inserted “Thus, for interval I a time of deposition of 433 ka is calculated,...” to clarify this calculation step.
Page 10, lines 21-23 p. 7682, line 11	We have added the sentence “The sedimentation rates from LR04 tie points were averaged over the length of the intervals and show mean values of 35 cm/ka for interval I and 48 cm/ka for interval II (Fig. 4).” and have changed Fig. 4 because we think that mean values of sedimentation rates from LR04 tie points can be compared much easier to sedimentation rates from sliding window.
Page 10, line 24-25 p. 7682, line 13	We have replaced “stretched GR data” by “GR data on decompacted depth-scale” to make our approach more comprehensible.
Page 11, line 10 p. 7683, line 2	We have corrected the numbers according to Fig. 5b.
Page 11, line 20 p. 7683, line 11	We have changed “Response of GR to the global climate” to “Climate response of GR...” to make clear that we have focused on Lake Ohrid’s climate.
Page 12, line 23 p. 7684, line 22	We have inserted “... lead or lag effects of the...” to be more precise.
Page 13, line 1-3 p. 7685, line 3	We have deleted “...decrease towards the top (wavelength of 45 m; starting from interval II).” and have inserted “... be higher in interval I (wavelength of 30 m) in comparison to interval II (wavelength of 45 m).” because it is easier to understand.
Page 13, line 13-14 p. 7685, line 14-15	We have deleted “The sedimentation rates ... (average of 48 cm/ka).” as we think that our statement is too generic and not helpful.
Page 13, line 15 p. 7685, line 16	We have corrected “MIS stages” to “MIS” and changed this throughout the article.
Page 13, line 28-30 p. 7686, line 1-3	We have added more information about the construction of the age-depth model from cores because we think that this information is required to justify our comparison.
Page 14, line 3-4 p. 7686, line 6-8	We have deleted “The averaged ... (mean of 32 cm/ka).” because it is not helpful to compare the results from both approaches at this point.
Page 14, line 23-26 p. 7686, line 26	We have inserted: “Underestimation of sedimentation rates from sliding window method is supported by comparison of results from LR04 tie points;

the latter indicate generally higher sedimentation rates (35 cm/ka; interval I and 48 cm/ka; interval II) and show very good agreement with the estimates of the effect of compaction. “, because this aspect complements our results.

Figures

- Fig. 1 We have labelled the top part of Fig. 1 with a) and the bottom part with b).
- Fig. 2 b) We have changed “tephra pointers” into “tephra tie points”.
- Fig. 2 c) We have deleted the left part of the figure, because the synthetic curve is also displayed in the right part of Fig. 2 c).
- Fig. 3 We have split Fig. 3 into a), b) and c).
- Fig. 4 We have removed the blue coloured areas, to be consistent with Fig. 2. Furthermore we have added the red dashed line “LR04 tie points, mean” to display average sedimentation rates from LR04 tie points.
- Fig. 5 b) We have changed “present thickness” into “present layer thickness” and “original thickness” accordingly.
- Fig. 5 c) We have changed the colour of intervals I and II to help to distinguish in between them and have modified the boxplot.
- Fig. 6 We have added a legend.

Figure captions

- Page 25, line 30-31 We have complemented the caption of Fig. 3 a) by “The dashed line separates the spectral background from the spectral peaks.”.
- Page 26, line 5-7 We have added “The dashed red line indicates the mean values of the sedimentation rates from LR04 tie points for interval I and II.” according to the modifications of Fig. 4.

Age-~~Age~~-depth-~~model~~ ~~for~~ ~~of~~ the past 630 ka ~~in~~ ~~for~~ Lake Ohrid (Macedonia~~FYROM~~/Albania) based on cyclostratigraphic analysis of downhole gamma ray data

H. Baumgarten¹, T. Wonik¹, D.C. Tanner¹, A. Francke², B. Wagner², G. Zanchetta³, R. Sulpizio⁴, B. Giaccio⁵, S. Nomade⁶

[1]{Leibniz Institute for Applied Geophysics, Hannover, Germany}

[2]{University of Cologne, Institute for Geology and Mineralogy, Cologne, Germany}

[3]{University of Pisa, Dipartimento di Scienze della Terra, Pisa, Italy}

[4]{University of Bari Aldo Moro, Dipartimento di Scienze della Terra e Geoambientali, Bari, Italy}

[5]{Istituto di Geologia Ambientale e Geoingegneria – CNR, Roma, Italy}

[6]{Laboratoire des Sciences du Climat et de l'Environnement, IPSL, laboratoire CEA/CNRS/UVSQ, Gif-Sur-Yvette, France}

Correspondence to: H. Baumgarten (Henrike.baumgarten@liag-hannover.de)

Abstract

Gamma ray (GR) fluctuations and potassium (K) values from downhole logging data obtained in the sediments of Lake Ohrid from 0 to 240 mblf correlate with fluctuations in $\delta^{18}\text{O}$ values from the global benthic isotope stack LR04 (Lisiecki and Raymo, 2005). GR and K values are considered a reliable proxy to depict glacial-interglacial cycles, with high clastic input during cold and / or drier periods and high carbonate precipitation during warm and / or humid periods at Lake Ohrid. We report the gamma ray fluctuations from downhole logging data obtained in the sediments of Lake Ohrid from 0 m to 240 m below lake floor. These variations in gamma ray and potassium values strongly correlate with fluctuations in global $\delta^{18}\text{O}$ values and can be thus considered a reliable proxy to depict glacial-interglacial cycles, with high elastic input during cold and / or drier periods and high carbonate precipitation during the warm and / or humid periods in Lake Ohrid. Spectral analysis (sliding window) was applied to investigate the climate signal and their evolution over the length of the borehole. Linking

~~the~~ downhole logging data with orbital cycles was used to estimate sedimentation rates and the effect of compaction was compensated for, ~~which shift from 45 cm/ka between 0 m to 110 m to 30 cm/ka from 110 m to 240 m below lake floor. The effect of compaction was compensated for.~~ Sedimentation rates increase on average by 14 % after decompaction of the sediment layers and the mean sedimentation rates shift from 45 cm/kyr between 0 to 110 m to 30 cm/kyr from 110 to 240 m below lake floor. Tuning of minima and maxima ~~in~~ of gamma ray and potassium values versus LR04 ~~minima and maxima~~ extrema, in combination with eight independent tephrostratigraphical tie points, allows ~~the establishment~~ establishing of a robust age model for the downhole logging data over the past 630 ka ~~in Lake Ohrid.~~

1 Introduction

Lake Ohrid is located at the border between the former Yugoslav Republic of Macedonia (FYROM) and Albania (40°70' N, 20°42' E) in the Central Mediterranean region (Fig. 1a). It is considered as one of the oldest, continuously-existing lakes worldwide. Its sediments are assumed to contain the climate history over more than one million years and numerous endemic species have evolved in Lake Ohrid. Several pre-site studies between 2004 and 2012, such as (e.g. multichannel seismic and shallow coring,) demonstrated the potential of Lake Ohrid to yield a complete and continuous paleoclimatic record (e.g., Wagner et al., 2008; Lindhorst et al., 2015). Hydroacoustic data obtained by multichannel airgun and sediment echosounder seismics revealed undisturbed sediments as well as certain high amplitude reflectors, which were interpreted as tephra layers (Lindhorst et al., 2015). A successful deep drilling campaign by the International Continental Scientific Drilling Program (ICDP) was performed in 2013. At the main drill site, the “DEEP site” in the central deep basin of Lake Ohrid (Fig. 1b), multiple coring and downhole logging tools were applied. ~~Hydroacoustic data obtained by multichannel airgun and sediment echosounder seismics revealed undisturbed sediments as well as certain high amplitude reflectors, which were interpreted as tephra layers~~

The reconstruction of Lake Ohrid’s climatic, tectonic and evolutionary biological history, is one of the key objectives of the project Scientific Collaboration on Past Speciation Conditions in Lake Ohrid (SCOPSCO) ~~project~~. This requires a reliable temporal framework of the biotic and abiotic events and thus the establishment of a robust age-depth age-model. This can be achieved by tephrostratigraphy (Sulpizio et al., 2010; Vogel et al., 2010c), the use of radiometric ages (e.g. from dating of volcanic material in the cores), or by tuning proxy data,

~~such as (e.g. $\delta^{18}\text{O}$ or TOC_2)~~ to reference records (Lang and Wolff, 2011; Stockhecke et al., 2014a). Suitable material for independent ~~dating-dating,~~ (e.g. well-preserved and coarse-grained tephra layers~~),~~ is often rare ~~in sediments~~ or hard to detect in sediments. Even if age control points are available, changes in the sedimentation rate between these points ~~is-remains~~ an uncertain interpolation. Amongst proxy data, the effect of global climate signals (Milanković cycles; Milanković, 1920) can be used to construct the temporal framework of a sedimentary record (Batenburg et al., 2012; Prokopenko et al., 2006; Wu et al., 2012). These cycles have periodicities of 100 ~~kyr~~ (eccentricity; E), 41 ~~kyr~~ (obliquity; O), 23 ~~ka~~ and 19 ~~kyr~~ (precession; P_2 , P_1) and determine the intensity of the solar insolation on Earth, whereas their effect is non-uniform and depends on the location of a certain site (e.g. the effect of O is strongest at polar regions) (Pälike, 2005). The 100 ~~kyr~~ cycle dominates the past c. 900 ka (Berger and Loutre, 2010), which is evident in sedimentary records and strongly imprinted in the widely-used global climate reference record (LR04-stack from benthic foraminifera $\delta^{18}\text{O}$) (Lisiecki and Raymo, 2005, 2007). To apply cyclostratigraphic methods successfully, generation and preservation of cycles is required, as well as their continuous recording. Such conditions are favoured in marine environments and ice cores, which are commonly used to analyse cyclicities (Barthes et al., 1999; Golovchenko et al., 1990; Jarrard and Arthur, 1989; Jouzel et al., 2007; Molinie and Ogg, 1990a). However, several lacustrine sequences have also recorded global climate signals and have been used for cyclostratigraphic studies (Baumgarten and Wonik, 2014; Bogota-A et al., 2011; Nowaczyk et al., 2013; Prokopenko et al., 2006). Whereas the majority of studies were performed on proxies from sediment cores (e.g. $\delta^{18}\text{O}$, organic matter or pollen), analysis of physical properties from downhole logging have also been ~~proven~~ successful (Barthes et al., 1999; Golovchenko et al., 1990; Jarrard and Arthur, 1989; Molinie and Ogg, 1990b; Wonik, 2001).

Physical in-situ properties ~~(e.g. seismic velocity or spectral gamma ray)~~ can be only achieved by downhole logging methods and provide a first data set that is available within hours after the tools are run in hole. Contrasting physical properties and therefore changes in the sediment characteristics (e.g. sedimentological composition, grain size) can trigger cyclic changes in the logging data (Baumgarten and Wonik, 2014; Kashiwaya et al., 1999; Paulissen and Luthi, 2011; Scholz et al., 2011). Such cyclic changes can ~~be~~ potentially be revealed by applying cyclostratigraphic methods. The aim of this study is the generation of a robust age depth-modelage-depth model down to 240 metres below lake floor (mblf) by an integrated study of downhole data with tephrostratigraphic age control from the sediment cores. Special emphasis is given to the effect of compaction and its subsequent impact on estimates of

sedimentation rates. Furthermore, the response of the physical in-situ properties from spectral gamma ray (contents of potassium, thorium and uranium) and their application as proxy for changing environmental conditions in the catchment area is investigated.

2 Setting and sediment dynamics of Lake Ohrid

Lake Ohrid is located on the Balkan Peninsula at an altitude of 693 m above sea level in a northwest-trending active tectonic graben. It is considered to have formed within a 1st stage ~~in~~ (Late Miocene) as a pull-apart basin and during a 2nd stage (~~in~~ Pliocene) of E-W extensional movement (E-W extension) which led to the recent geometry (Lindhorst et al., 2015). The lake is considered to be the oldest continuously-existing lake in Europe, as supported by molecular clock analysis that estimate the onset of the lake formation to 1.5 to 3 ~~million years~~ (Ma) (Trajanovski et al., 2010; Wagner et al., 2014). It houses an extraordinary number of endemic species (> 200, e.g. ostracodes), and it is therefore considered to be a hotspot to study the evolution of the various species (Albrecht and Wilke, 2008).

Oligotrophic Lake Ohrid has a surface area of 360 km² and a water depth of up to 290 m. The water originates mainly from karst inflows (50%), precipitation (25%), and ~~river and~~ surface runoff (25%), ~~whereas~~ the karst springs are primarily fed by the ~~150 m higher~~ “sister lake” Prespa, 150 m higher in elevation (Wagner et al., 2014). The recent local climate is characterized by warm dry summers (mean temperature 26°C) and cold winters (-1°C). The annual precipitation is about 750 mm and ~~the~~ winds are prevailing southerly or northerly, which is topographically controlled by the shape of the lake valley basin (Vogel et al., 2010a).

Due to its downwind location of most of the Quaternary volcanoes of central-southern Italy, Lake Ohrid’s sediments can provide a record of the volcanic history of the northern Mediterranean region (Sulpizio et al., 2010). ~~The oligotrophic lake houses an extraordinary number of endemic species (>200, e.g. ostracodes) and it is therefore considered to be a hotspot to study the evolution of the various species.~~ The catchment area southeast and northwest of the lake mostly consists of Triassic carbonates and clastics, whereas ophiolites (nickel, iron and chromium-bearing) are exposed on the western and southwestern shore (Vogel et al., 2010b).

The sediment dynamics for the past 150 ka have been investigated by up to 15 m long sediment cores from different marginal parts of the lake basin (e.g. Wagner et al. 2009, Belmecheri et al., 2009, Vogel et al., 2010a). ~~To simplify,~~ two major lithofacies ~~can be~~ are

distinguished: A) sediments with high detrital clastic content with no or very low carbonate content, together with low ~~total~~ organic matter and few diatoms, and B) sediments with high content of carbonates, abundant ostracodes, ~~small-minor amounts of~~ clastics and high ~~contents of~~ organic matter. Lithofacies A is associated with glacial conditions (Marine Isotope Stages; MIS 2, 4, 6), high clastic supply and low lake productivity, whereas lithofacies B formed during interglacial conditions (mainly during MIS 1 and 5), with high lake productivity and formation of authigenic carbonates. Age control of the ~~last glacial cycle~~ sediments was obtained by radiocarbon dating and tephrochronology.

3 Methods and background

3.1 Downhole logging data acquisition and processing

The multiple-cored DEEP site has six ~~parallel and overlapping~~ boreholes (A to F), of which holes A and E only cover the uppermost few meters of the sediment succession. Each of the deeper holes was drilled with a diameter of 149 mm and water-based mud was used to clean the holes from cuttings and to stabilize the side walls during the coring process. Hole C was logged immediately after drilling down to 470 mblf, and amongst other probes, ~~such as (e.g. resistivity and borehole televiewer)~~, spectral gamma ray (SGR) and sonic were used. To prevent the unconsolidated sediments ~~from~~ caving in, the SGR probe was run through the drillpipe and a continuous record of the sediments down to 470 mblf was achieved. The SGR data was acquired using the SGR 70-slimhole tool of the Leibniz Institute for Applied Geophysics (LIAG), which records the total gamma radiation (GR), as well as the spectral components (potassium; K, thorium; Th and uranium; U) and their contribution to the GR. The tool was run with a logging speed of 3 m/min and a sampling rate of 10 cm. The achievable minimum bed resolution is controlled by the size of the ~~Bismuth germinate (BGO)~~ crystal (5 x 15 cm) and the characteristics of the target formation ~~(e.g. such as the absolute value range and contrast of values between neighbouring beds)~~ (Theys, 1991). The vertical resolution can be estimated ~~at-to~~ 15 - 20 cm. The sonic tool, which measures the seismic velocity (V_p), was applied afterwards at a speed of 4 m/min and a depth increment of 10 cm. To allow open hole logging by sonic, the drillpipes were successively pulled upwards until open hole sections of c. 50 m were accessible. The uppermost 30 mblf could not be logged by the sonic tool, because some drillpipes were kept in hole to allow other probes to enter. The measuring principles are described by Rider and Kennedy (2011) and the tools are specified in Buecker et al. (2000) and Barrett et al. (2000). The data was acquired, preprocessed and

processed with the software GeoBase® (Antares, Germany) and WellCAD® (Advanced Logging Technology, Luxembourg).

3.2 Sliding window method

Sedimentary cycles in lake records can be studied by cyclostratigraphic methods for a potentially orbital driven origin (Lenz et al., 2011; Prokopenko et al., 2001; Weedon, 2003). To investigate wavelengths and amplitude of the contained signals, fast Fourier transform (Weedon, 2003) can be ~~used~~applied. The sliding window method (\equiv windowed Fourier transform) (Baumgarten and Wonik, 2014; Molinie and Ogg, 1990b; Torrence and Compo, 1998; Weedon, 2003) can be applied to identify the distribution of cycles within a series and their evolution over the dataset: the spectral analysis is calculated for a depth interval of specific length (window size) and the resulting spectrum is allocated to the centre of the window. Subsequently, the window is moved downwards by a certain step size and the analysis is repeated at consecutive depth positions until the window border reaches the end of the dataset. The results are presented in a three-dimensional spectrogram with colour-coding of the relative power of the different frequency components. Generally, a small window size is favourable to maximize the length of the resulting plot. However, the contained cycle needs to be covered and cannot be determined if the window size was chosen too short, e.g. only half the signal's wavelength. The optimal window size ~~can be~~is determined by empirical testing. Spectral analysis for identification of the characteristic periodicities (Jenkins and Watts, 1969; Priestley, 1981) was performed on normalized SGR data using fast Fourier Transform within MATLAB (MathWorks®).

The detection of cycles by SGR logging is limited by the Nyquist Frequency, ~~(twice the sampling rate)~~ (Molinie and Ogg, 1990a). The temporal resolution can be estimated by the vertical resolution of the applied tools ~~(minimum bed resolution of the SGR tool of 15–20 cm; section 2.1)~~ and the averaged sedimentation rate. For a mean sedimentation rate of e.g. 38 ~~cm/kacm/kyr~~, cycles in the range of 0.8 to 1.1 ~~kakyr~~ are resolvable by SGR logging.

3.3 Depth matching of downhole logging and core data

In this workstudy, downhole logging data, in conjunction with stratigraphically aligned tephra layers in the cores~~age control points from tephra layers~~, is used to construct an age-age-depth-model. Therefore, matching of core and logging depth is required. To provide age control by distinct tephra layers, they need to be identified in the cores by visual description or by their physical properties, such as ~~(e.g. susceptibility from core logging,)~~ in contrast to the background sedimentationsediments. Artifacts in the coring process as incorrect depth

allocation of coring tools or gas extension of sediments after cores are on deck and pressure release produce erroneous depth. Furthermore, depth shifts between core and logging depth are generated because the downhole data originates from one hole (C; down to 470 mblf) and the core composite record (see Francke et al.; [this issue 2015](#)) is composed of four different holes ([section 2.1](#)) which are tens of metres apart. The depth of a distinct sediment layer may differ up to 3 to 4 m between these holes. The matching of borehole logging data and sediment core is described in detail in Francke et al. ([this issue 2015](#)) and is based on a correlation of K₂O contents from SGR with K₂O intensities from [x-ray fluorescence \(XRF\)](#)-scanning, and using magnetic susceptibility from downhole logging and Multi Sensor Core Logging (MSCL) on sediment cores. Trends and patterns were compared and [matched; the larger features were](#) preferred over correlation of [\(single\)](#)-small-scaled features in the data. Cross correlation was used to prevent systematic depth shifts of these data sets and for quality control.

3.4 Compaction

To perform cyclostratigraphic studies and to estimate an [age-age-depth-](#)relationship and sedimentation rates, compaction and associated reduction of sediment thickness due to overburden pressure must be considered. The original (decompacted) thickness of the sediments can be calculated if the initial (surface) porosity and the compaction coefficient (Brunet, 1998) can be determined. The amount of porosity decrease with greater depth depends on sediment properties, [e.g. such as](#) grain size and sorting (Serra and Serra, 2003) and can be expressed as:

$$\Phi(z) = \Phi_0 * e^{(-cz)}$$

_____ Eq. (1)

where the porosity ($\Phi(z)$) at a specific depth (z) is to be estimated; Φ_0 is the initial porosity and c is the compaction coefficient (Athy, 1930; Brunet, 1998).

[Whereas](#) [p](#)Porosity can be measured directly on the sediment cores, e.g. by Archimedean weighing, [Whereas](#) the physical properties, in particular from (unconsolidated) sediment cores are typically disturbed due to drilling, release of pressure, and core handling. Therefore, measurements by downhole logging are more suitable; in-situ porosity can be gained by neutron porosity logging or derived, e.g. from bulk density. These tools operate with radioactive methods and the import procedure into foreign countries is usually extremely complicated and seldom successful. Therefore, the radioactive tools from the LIAG could not

be used at Lake Ohrid. However, porosity was derived by an empirical relationship from sonic data (Vp) (Erickson and Jarrard, 1998), which were recorded continuously from below 30 mblf. The software 2DMove® (Midland Valley Exploration Ltd.) was used to decompact the sediments and calculate the original sediment thickness.

4. Results

4.1 Selection of SGR data

The output curves from SGR were compared to estimate the contribution of the spectral components to the total gamma ray. GR is mainly controlled by K and Th, which develop uniformly ($R > 0.9$). GR and K were used for further investigations, ~~whereas~~ K was chosen over Th, because it is also available from XRF core scanning and the interpretation can be reviewed easily.

4.2 Correlation of GR with the global climate reference $\delta^{18}\text{O}$ record

The downhole logging data (GR and K) ~~between from~~ 0 m and 240 mblf was compared to the global benthic isotope stack LR04 ~~stack~~ (Lisiecki and Raymo, 2005). In order to select an appropriate temporal window we considered the current age estimates from ~~tephra dating~~ stratigraphical aligned tephra layers (eight age-depth points; table 1). After the anchor points from tephra deposits were defined, significant variations in the data were correlated; a very similar cyclicity with a positive correlation between GR and K from downhole logging data and $\delta^{18}\text{O}$ data was observed (Fig. 2a). The onset and terminations of several MIS ~~stages~~ can be easily distinguished in the downhole logging data, whereas warm and / or humid periods (decreased $\delta^{18}\text{O}$ values) correlate with low GR values. 30 additional tie points (~~Table-table~~ 1) were set due to the strong similarities between the curves characteristics. After matching these tie points, high correlation of both datasets ($R = 0.75$) was observed. The tephra ages and tie points from correlation between GR, K and LR04 were used to assign a (preliminary) age-time scale to the data (Fig. 2b). Within the data, the age-time scale between the tie points was generated by linear interpolation. According to the established age model, the 240 m long sediment succession covers a time period between ~~e-~~ 630 ka (including MIS 15) and the present.

The conspicuous similarity of the datasets allows calculation of a synthetic $\delta^{18}\text{O}$ -curve from GR by a ~~simple~~-regression of both datasets. Therefore, normal-distributed data is required and

thus the prominent tephra layers at 20 and 68 mblf (Fig. 2c) were considered to be outliers and removed. Best results were achieved by a linear solution ($R^2 = 0.60$) as follows:

$$\delta^{18}\text{O}_{\text{calc.}}(\text{‰}) = 3.19 + 0.03 * \text{GR (gAPI)} \quad \text{Eq. (2)}$$

~~$$\delta^{18}\text{O}_{\text{calc}}(\text{‰}) = 3.19 + 0.03 * \text{GR(gAPI)} \quad \delta^{18}\text{O}_{\text{calc}}(\text{‰}) = 3.19 + 0.03 * \text{GR(gAPI)}$$~~

Whereas cycles and trends are similar in both datasets, the amplitudes between the LR04 stack and the synthetic $\delta^{18}\text{O}$ (derived from GR; $\delta^{18}\text{O}_{\text{calc}}$; Fig. 2c) are not completely matched. The $\delta^{18}\text{O}_{\text{calc}}$ values from 630 to 430 ka are lower than compared to LR04. From 430 ka to 185 ka the amplitude of $\delta^{18}\text{O}_{\text{calc}}$ is higher and during the past 185 ka, $\delta^{18}\text{O}_{\text{calc}}$ is mostly decreased compared to LR04. These three zones (A to C) are indicated in Fig. 2c.

4.3 Spectral characteristics of GR data, temporal evolution and sedimentation rates

After visual comparison of GR and K ~~and with~~ LR04 ~~documenting a and the observed~~ strong correlation of periods with low GR and K ~~and with~~ warm and / or humid periods, the application of spectral analysis by sliding window method ~~(section 3.2) was applied to~~ objectively ~~identify-identifies~~ the possible cycles and their temporal distribution. The spectral analysis was calculated with a window of 90 m length and a step size of 1 m. Thus, the stepwise calculation for the depth section from 0 to 240 mblf and the resulting three-dimensional spectral plot (Fig. 3a) is composed of 150 spectra. The plot ranges from 45 to 240 mblf, because the first spectrum is allocated to the window centre (section 3.2) and therefore, half of the window length is not displayed. Two prominent spectral peaks are evident in the dataset, as indicated by colour. ~~These spectral peaks have~~ with wavelengths of 30 ~~m~~ and 45 ~~m~~ ~~(Fig. 3)~~. The distribution of the cycles is non-uniform ~~over~~ along the dataset and a break in the spectral characteristics occurs at about 110 mblf. Based on the reduced relative power of the 30 m signal and the subsequent increased power of the 45 m frequency at 110 mblf, the plot can be split into a lower interval ~~(I)~~ and an upper interval ~~(II)~~ (Fig. 3a). In addition, ~~Two~~ single spectra from depths of 170 and 50 mblf ~~(Fig. 3b, c) are displayed in~~ Figure 3.

The similar cyclicity in the LR04 stack and GR (Fig. 2a, ~~2b~~) suggests that the 100 ~~ka~~ kyr cycle, known as dominant periodicity in sedimentary archives for the past c. 900 ka ~~and~~ clearly ~~documented~~ written in the $\delta^{18}\text{O}$ data, has the strongest effect on the cyclic characteristics of the GR data. The highest amplitudes were therefore linked to the 100 ~~ka~~ kyr cycle. Averaged sedimentation rates can be calculated using this link (45 m \equiv 100 ~~ka~~ kyr cycle), for 110 to 0 mblf as follows:

$$\frac{45 \text{ m}}{100 \text{ ka}} = 45 \frac{\text{cm}}{\text{ka}}$$

$$\underline{45 \text{ m} / 100 \text{ kyr} = 45 \text{ cm/kyr}}$$

Eq. (3)

Furthermore, the time of deposition can be estimated by using this sedimentation rate and the length of the interval II (length of 110 m):

$$\frac{110 \text{ m}}{45 \frac{\text{cm}}{\text{ka}}} = 244 \text{ ka.}$$

$$\underline{110 \text{ m} / 45 \text{ cm/kyr} = 244 \text{ ka}}$$

Eq. (4)

The sedimentation rate for interval I (length of 130 m) can be calculated as 30 cm/ka (30 m \equiv 100 ka cycle). Thus, for interval I the duration of deposition of 433 ka is calculated. -which gives an overall time of deposition (sum of interval I and II) of 677 ka.

The sedimentation rates from sliding window show a distinct shift from 30 cm/ka to 45 cm/ka at e-110-mblf (Fig. 4). However, the sedimentation rates from visual tying to LR04 are much more variable and range from 22 to 71 cm/ka. Exceptionally high sedimentation rates occurred during MIS 6 and lowest sedimentation rates occurred during MIS 11 and 13. The sedimentation rates from LR04 tie points were averaged over the length of the intervals and show mean values of 35 cm/kyr for interval I and 48 cm/kyr for interval II (Fig. 4).

4.4 Decompaction of the pelagic sediments and subsequent spectral analysis on stretched GR data on decompacted depth scale

The effect of decreased sediment thicknesses due to compaction over time was determined to investigate its impact on the estimates of sedimentation rates. The Vp data from sonic logging was used to derive porosity after Erickson and Jarrard (1998). The porosity values were averaged for layers of 100 m thickness (Fig. 5a). The initial porosity (ϕ_0) was determined at 80-% and the compaction coefficient was estimated at 0.39 km^{-1} . These parameters were used as input data for modelling decompaction of the sediments, and the 2D model was calculated for layers of 50 m thickness. The modelling process starts with the removal of the top layer and subtraction of its overburden pressure. The new thicknesses of the lowermost layers are thereafter calculated and these steps were repeated again downwards. The resulting thicknesses of the sediment layers after decompaction show a quasi-linear increase with

greater depth for these small depths (Fig. 5b). ~~The~~ decompaction of the sediment layers ranges from 10 to 30% downwards and the cumulative thickness of the sediment sequence (present thickness of ~~240-250~~ m) is increased by ~~36-35~~ m (to ~~276-285~~ m).

The GR data was stretched (Fig. 5c) and subsequently spectrally analyzed by sliding window (Fig. 5d) to determine the effect of decompaction on the spectral analysis. The spectral analysis shows two spectral peaks (Fig. 5d; wavelength of 36 m from 276-~~m~~ to 118 m and wavelength of 48 m from 118 ~~m~~ to 0 m). Linking these spectral peaks to the 100 ~~ka~~ kyr cycle provided sedimentation rates of 36 ~~cm/ka~~ cm/kyr for interval I and 48 ~~cm/ka~~ cm/kyr for interval II. Times of deposition remain constant and are 433 ka for interval I and 244 ka for interval II, respectively.

5. Discussion

5.1 Climate Response of GR ~~to the global climate~~ over the past 630 ka

The strong correlation of GR and K with LR04 (low GR and K during warm and / or humid periods, high in cold and / or drier periods) suggest a response of the sedimentary system to the temperature and hydrological changes related to the global ice-volume fluctuations ~~of~~ during the glacial-interglacial cycles. The fluctuations are likely to be controlled by the input and deposition of clastics (K and Th sources), which are suggested to have increased during the past c. 136 ka, when glacial conditions prevailed (except MIS 1 and 5e) at Lake Ohrid (Vogel et al., 2010a). In particular, the reduced input of organic matter and calcium carbonate during cold and / or drier periods seems to amplify the enhanced input of clastic material. During warm and / or humid periods, carbonate production and preservation is increased (Vogel et al., 2010a). In combination with higher organic matter flux, the clastic content of the sediments is reduced and the GR and K data is lower. Either the total content of clastics is lower during warm-humid periods or the amount is decreased ~~relatively to~~ relatively to carbonate ~~(and organic matter diluted)~~. However, as discussed by Vogel et al. (2010a), less vegetation cover during cold-drier periods is likely and also suggests increased erosion in the catchment and subsequent higher input of clastic material. Based on our interpretation, these ~~dynamics of a~~ cyclic changes of from carbonate-rich and to clastic-rich sedimentation were constant at least for the past 630 ka, ~~as evident in the GR and K data~~.

Three zones were observed, based on ~~difference in the~~ amplitude differences between the synthetic $\delta^{18}\text{O}$ curve from GR ($\delta^{18}\text{O}_{\text{calc}}$) and the referenced record: A) 630-~~ka~~ to 430 ka (MIS

15 to MIS 12), B) 430 ka to 185 ka (MIS 11 to MIS 7) and, C) 185 ka to 0 ka (MIS 6 to MIS 1). ~~The eC~~ comparison of the synthetic $\delta^{18}\text{O}_{\text{calc}}$ to ~~the~~ LR04 revealed systematically lower values in zones A) and C) and higher values in zone B). ~~Under the assumption that our data reflects prevailing climate-driven fluctuations in the sediments, the differences between the $\delta^{18}\text{O}_{\text{calc}}$ and LR04 could indicate deviations from a linear response to the global ice volume fluctuations. Therefore, the suggested climate signal would not completely be in line with the global climate variations and be more variable even on glacial-interglacial scale. Furthermore, local environmental processes (e.g. variations in the catchment area due to topographic changes and subsequent supply of elastics) might have additionally affected the sediment properties. The (few) tephra deposits have contributed to the characteristics of the data as well; the tephra layers can be recognized in the K data and have shaped the curve, in addition to the climate-dependent deposition of elastics.~~

We suggest the following reasons of the GR signature:

1) Climate dependent supply and deposition of K-rich clastics (feldspars, clays). They are increased during cold-dry periods (high GR) and decreased during warm-wet periods (high carbonate deposition; low GR) in the sediments.

2) Tephra layers that are partly recognizable in the GR / K data (increased GR). Even if the prominent layers at 20 and 68 mblf could be removed, at least 6 additional tephra layers (see tephra tie points; Fig. 2b) were identified in the cores down to 240 mblf. These thin layers (thickness < 10 cm) are not recognizable easily in the GR data and could not be removed but are assumed to contribute to the GR / K curve. Their occurrence in zones A and C (Fig. 2c; zones of decreased synthetic $\delta^{18}\text{O}$) suggest that they have an effect on the GR signature.

3) Variations in the catchment area. Outcrops of Triassic carbonates and clastics occur in large parts in Lake Ohrid's catchment area. Furthermore, ophiolites, magmatic and metamorphic rocks are exposed and are potential sources of terrestrial material. Erosion and transport of these rocks, e.g. by means of surface runoff into the lake, was likely variable over time and subsequently the input of K-bearing particles.

Therefore, the GR is most likely controlled by several factors and cannot be described in total by linear solution. However, the main component seems to be a linear response of K-rich sediments to the global climate trend (1). Further, we consider the attempt useful to compare

both datasets and to show the very unusual similarity in cyclic characteristic between LR04 and GR.

~~The~~ matching of ~~the~~ GR and K data with the global climate reference record (LR04) equates the timing of the climate dynamics recorded in the oceans to Lake Ohrid. This means that if the downhole logging data is tied to this age-time scale, differences between the response times of Lake Ohrid and the global climate trend (e.g., lead or lag effects of the onset of terminations) ~~could be~~ lost. However, even if the comparable small system was likely to be subject to a faster climate response compared to records from the marine sediments realm, ~~the~~ correlation with the global signal and the resulting age-age-depth- model ~~can be still~~ is verified in large parts (down to 206 mblf) by tephrochronology. ~~Further interpretation of the complete dataset was postponed to allow integrated investigation of cyclostratigraphic analysis with age control from cores.~~

5.2 Sedimentation rates: major trends, small-scale fluctuations and the effect of compaction

The relative power of the spectral peaks from sliding window analysis seems to be higher in interval I (wavelength of 30 m) in comparison to interval II (wavelength of 45 m) ~~decrease towards the top (wavelength of 45 m; starting from interval II).~~ The strength of the signal depends on the number of cycles that are detected by spectral analysis. The 45 m long cycle can be contained up to 2.4 times in the 110 m long interval II, whereas the cycle of wavelength of 30 m might be recorded more frequently (4.3 times) in the 130 m long interval (I). This might can contribute to the higher intensity of the 30 m amplitude and thus we cannot interpret ~~this as a~~ stronger cyclicity in for the lower part.

Based on sliding window analysis the sedimentation rates are constant (30 cm/kacm/kyr) for a long period of time (433 ka), apart from a shift to increased rates at about 110 mblf to 45 cm/kacm/kyr. However, small-scale variations ~~in these rates~~ cannot be resolved due to averaging and the used window of 90 m length. More variable and realistic results are indicated by tying of GR and K to LR04. ~~The sedimentation rates are generally lower from MIS 15 to MIS 9 (average of 32 cm/ka) and higher from MIS 8 to 1 (average of 48 cm/ka).~~ The lowest rates (minimum of 22 cm/kacm/kyr) occur during MIS ~~stages~~ 13, 11 and 9. Strongly- increased sedimentation rates (up to 71 cm/kacm/kyr) occur during MIS 8 and in particular during MIS 6. Therefore, ~~a tendency of~~ decreased sedimentation rates during interglacials and increased rates during glacial periods can be derived. Even if these fluctuations do not correlate with all ~~of the MIS stages~~, it they seems to be largely coupled to

glacial-interglacial dynamics ~~in large parts~~. This trend suggests higher accumulation of clastic-rich glacial deposits compared to calcium carbonate-rich deposition during interglacials. The overall trend from lower mean rates in the bottom part (> 110 mblf, sliding window; > 130 mblf; LR04 tie points) to increased values towards the top is comparable.

The cumulative time of deposition based on these sedimentation rates and ~~the~~ corresponding sediment thicknesses range from 630 ka (~~visual-LR04~~ tie points) to 677 ka (sliding window method) and are overall in a similar range (Fig. 6). We consider the estimated time of deposition from the tuning to LR04 to be of higher accuracy ~~than~~ compared to the averaged estimates from sliding window analysis. The agreement with results-age estimates from cores, based on wiggle matching of (bio-) geochemistry data, such as XRF scanning data, to LR04 and local insolation patterns (Francke et al., 2015), (Francke et al., this issue) supports the age-age-depth-model-in-addition. Nonetheless, the sliding window method is proven useful to estimate averaged sedimentation rates and to provide complementary complements the results of the cyclic characteristics of the data. Whereas age control from tephrachronology is only available only down to 206 mblf, the-our interpretation was extended down to 240 mblf based on the constant cyclic characteristics ~~at these depths~~. ~~The averaged sedimentation rates from sliding window (30 cm/ka) agree with the rates from tuning to LR04 (mean of 32 cm/ka).~~

The required initial porosity for modelling of the effect of compaction was derived from sonic logging ($\phi_0 = 80\%$) and is commonly lower (at c. 65%) for sedimentary basins. Studies of physical properties of marine sediment cores have shown comparable value ~~rangess~~ for seafloor deposits ($\phi = 80\%$, $V_p = 1540$ m/s; Kim and Kim, 2001) and even higher porosity values (> 80%; Kominz et al., 2011) for unconsolidated sediments. The compaction coefficient c was estimated at 0.39 km^{-1} and lies in a-value the range between cthat used for sands (0.20 km^{-1}) and carbonates (0.50 km^{-1}) and thus is considered as reasonable. The overall trend of a quasi-linear evolution of decompaction with increasing depth was observed, although Eq. (1) describes an exponential curve, it can be approximated to a line over short (~~<500 m~~) lengths (< 500 m). This is in accordance with the average linear increase of V_p with greater depth. The tephra layers, with only few cm thicknesses, are considered to have little impact on the compaction of these sediments.

~~The~~ spectral analysis on-of GR data on decompacted depth scale (Fig. 5 c) the stretched data set revealed a very similar spectral characteristic compared to the sliding window plot of the compacted data. However, the two spectral peaks (wavelengths of 30 ~~m~~ and 45 m) are shifted to higher wavelengths and increased to wavelengths of 36 m (for interval I) and 48 m (for

interval II). Therefore, the sedimentation rates are increased accordingly to 36 cm/kyr and would be underestimated by 7 to 20%, if they are not corrected for the effect of compaction. Underestimation of sedimentation rates from sliding window method is supported by comparison of results from LR04 tie points; the latter indicate generally higher sedimentation rates (35 cm/kyr; interval I and 48 cm/kyr; interval II) and show very good agreement with the estimates of the effect of compaction.

To ~~estimate~~determine the time of deposition, two input quantities were used: 1) ~~the~~ sedimentation rates and, 2) the thickness of the sediment layer for which they apply. Due to the stretching of the dataset, the resulting sedimentation rates, as well as the length of the intervals are increased and thus the ~~time of deposition~~duration of deposition remains unchanged. Therefore, the effect of compaction on this calculation is neglectable.

6. Conclusions

Can climatic indicators be derived from downhole logging, despite its limited vertical (and temporal) resolution and can these proxies be used to reconstruct a robust ~~age-depth~~modelage-depth model?

The strong response to the global climate signal (LR04) suggests that the K ~~(and Th)~~contents reflects a cyclic change of undisturbed, continuous sedimentation, ~~and thus that the~~ eConditions were constant over a long period of time and prevailing in balance with the global climate. To investigate the response of our data to the global climate trend, a synthetic $\delta^{18}\text{O}$ -curve was generated that reveals minor deviations compared to LR04. The deviations could indicate either that the local climatic conditions were not fully in line with the global climate or, that local processes in the sedimentary system changed over time.

Within two independent attempts, visual tying to the global reference LR04 record as well as spectral analysis by ~~the~~ sliding window method; and linking of high amplitudes to orbital cycles, a similar result was achieved. To derive sedimentation rates from ~~sliding windowspectral analysis-method~~, the effect of compaction must be taken into account. Our results show that tThe use of the present thicknesses of the sediment layers underestimates sedimentation rates by an average 14% ~~and these~~which needs to be corrected for by decompaction.

In conjunction with tephrochronology from the same core material, a robust ~~age-age~~age-depth-relationship model can be ~~created~~established.

This data set will play a crucial role for other working groups and will complement the ~~age-~~
~~depth-~~ model from core analysis ([Francke et al., 2015](#)). Their combination will provide the
temporal framework (~~e.g. for refining of the seismo-stratigraphical model by Lindhorst et al.~~
(2015)) and ~~will there within~~ contribute to the reconstruction of Lake Ohrid's climatic,
tectonic and evolutionary biological history ~~and to~~ answer the main research questions of the
SCOPSCP-SCOPSCO project.

Due to the successful construction of an ~~age-~~age-~~depth-~~ model based on the GR and K data
down to 240 mblf, we are optimistic that the complete lacustrine sediment succession (down
to 433 mblf) has high potential for cyclostratigraphic analysis and will provide a key
component to determine Lake Ohrid's temporal framework.

Acknowledgements

The SCOPSCO Lake Ohrid drilling campaign was funded by ICDP, the German Ministry of
Higher Education and Research, the German Research Foundation, the University of Cologne,
the British Geological Survey, the INGV and CNR (both Italy), and the governments of the
~~republics of Macedonia (FYROM)~~ and Albania. Logistic support was provided by the
Hydrobiological Institute in Ohrid. Drilling was carried out by Drilling, Observation and
Sampling of the Earth's Continental Crust's (DOSECC) and using the Deep Lake Drilling
System (DLDS). Special thanks are due to Beau Marshall and the drilling team. Ali Skinner
and Martin Melles provided immense help and advice during logistic preparation and the
drilling operation.

We thank the German Research Foundation for financial support (~~WO 672/10-1~~) for the
downhole logging (WO 672/10-1). The acquisition of these high quality data was only
possible due to the great commitment of our technical staff Thomas Grelle and Jens Kuhnisch.

References

- Albert, P.G., Hardiman, M., Keller, J., Tomlinson, E.L., Smith, V.C., Bourne, A.J., Wulf, S., Zanchetta, G., Sulpizio, R., Müller, U.C., Pross, J., Ottolini, L., Matthews, I.P., Blockley, S.P.E., Menzies, M.A. 2014. Revisiting the Y-3 tephrostratigraphic marker: a new diagnostic glass geochemistry, age estimate, and details on its climatostratigraphical context. *Quaternary Science Reviews*, in press 10.1016/j.quascirev.2014.04.002.
- Albrecht, C., Wilke, T., 2008. Ancient Lake Ohrid: Biodiversity and evolution. *Hydrobiologia* 615, 103-140.
- Athy, L.F., 1930. Density, porosity, and compaction of sedimentary rocks. *AAPG Bulletin* 14, 1-24.
- Barrett, P.J., Sarti, M., Wise, S., 2000. Studies from the Cape Roberts Project Ross Sea, Antarctica Initial Report on CRP-3 Terra Antarctica 7, 19-56.
- Barthes, V., Pozzi, J.P., Vibert-Charbonnel, P., Thibal, J., Melieres, M.A., 1999. High-resolution chronostratigraphy from downhole susceptibility logging tuned by palaeoclimatic orbital frequencies. *Earth and Planetary Science Letters* 165, 97-116.
- Batenburg, S.J., Sprovieri, M., Gale, A.S., Hilgen, F.J., Hüsing, S., Laskar, J., Liebrand, D., Lirer, F., Orue-Etxebarria, X., Pelosi, N., Smit, J., 2012. Cyclostratigraphy and astronomical tuning of the Late Maastrichtian at Zumaia (Basque country, Northern Spain). *Earth and Planetary Science Letters* 359–360, 264-278.
- Baumgarten, H., Wonik, T., 2014. Cyclostratigraphic studies of sediments from Lake Van (Turkey) based on their uranium contents obtained from downhole logging and paleoclimatic implications. *International Journal of Earth Sciences*, 1-16.
- Belmecheri, S., von Grafenstein, U., Namiotko, T., Robert, C.M., Andersen, N., Danielopol, D.L., Caron, B., Bordon, A., Regnier, D., Mazaud, A., Sulpizio, R., Zanchetta, G., Grenier, C., Tiercelin, J.J., Fouache, E., Lezine, A.M., 2009. Potential of Lake Ohrid for long palaeoclimatic and palaeoenvironmental records; the last glacial-interglacial cycle (140 ka). *Eos, Transactions, American Geophysical Union* 90, @AbstractPP14A-03.
- Berger, A., Loutre, M.F., 2010. Modeling the 100-kyr glacial-interglacial cycles. *Global and Planetary Change* 72, 275-281.
- Bogota-A, R.G., Groot, M.H.M., Hooghiemstra, H., Lourens, L.J., van der Linden, M., Berrio, J.C., 2011. Rapid climate change from north Andean Lake Fuquene pollen records

driven by obliquity; implications for a basin-wide biostratigraphic zonation for the last 284 ka. *Quaternary Science Reviews* 30, 3321-3337.

Brunet, M.-F., 1998. Method of quantitative study of subsidence. Oxford & IBH Publishing Company Pvt.: New Delhi, India, pp. 79-88.

Buecker, C.J., Jarrard, R.D., Wonik, T., Brink, J.D., 2000. Analysis of downhole logging data from CRP-2/2A, Victoria Land Basin, Antarctica; a multivariate statistical approach. *Terra Antarctica* 7, 299-310.

De Vivo, B., Rolandi, G., Gans, P.B., Calvert, A., Bohrsen, W.A., Spera, F.J., Belkin, H.E., 2001. New constraints on the pyroclastic eruptive history of the Campanian volcanic Plain (Italy). *Min. Pet.* 73, 47-65.

Erickson, S.N., Jarrard, R.D., 1998. Velocity-porosity relationships for water-saturated siliciclastic sediments. *Journal of Geophysical Research* 30,385 - 30,406.

[Francke, A., Wagner, B., Just, J., Leicher, N., Gromig, R., Baumgarten, H., Vogel, H., Lacey, J.H., Sadori, L., Wonik, T., Leng, M.J., Zanchetta, G., Sulpizio, R., Giaccio, B., 2015. Sedimentological processes and environmental variability at Lake Ohrid \(Macedonia, Albania\) between 640 ka and present day. *Biogeosciences Discuss.* 12, 15111-15156.](#)

Giaccio, B., Arienzo, I., Sottili, G., Castorina, F., Gaeta, M., Nomade, S., Galli, P., Messina, P., 2013a. Isotopic (Sr-Nd) and major element fingerprinting of distal tephras: an application to the Middle-Late Pleistocene markers from the Colli Albani volcano, central Italy. *Quaternary Science Reviews*, 67, 190-206.

Golovchenko, X., O'Connell, S.B., Jarrard, R.D., 1990. Sedimentary response to paleoclimate from downhole logs at Site 693, Antarctic continental margin. *Proceedings of the Ocean Drilling Program, Scientific Results* 113, 239-251.

[Hu, S., Goddu, S.R., Appel, E., Verosub, K., 2007. Fine tuning of age integrating magnetostratigraphy, radiocarbon dating, and carbonate cyclicity; example of lacustrine sediments from Heqing Basin \(Yunnan, China\) covering the past 1 Myr. *Journal of Asian Earth Sciences* 30, 423-432.](#)

Iorio, M., Liddicoat, J., Budillon, F., Incoronato, A., Coe, R.S., Donatella, D., Insinga, D., Cassata, W., Lubritto, C., Angelino, A., Tamburrino, S., 2013. Combined palaeomagnetic secular variation and petrophysical records to time constrain geological and hazardous events:

an example from the eastern Tyrrhenian Sea over the last 120 ka. *Global and Planetary Changes* 113, 91-109.

Jarrard, R.D., Arthur, M.A., 1989. Milankovitch paleoceanographic cycles in geophysical logs from ODP Leg 105, Labrador Sea and Baffin Bay. *Proceedings of the Ocean Drilling Program, Scientific Results* 105, 757-772.

Jenkins, G.M., Watts, D.G., 1969. *Spectral analysis and its applications*. San Francisco: Holden Day, 525 p.

Jouzel, J., Masson-Delmotte, V., Cattani, O., Dreyfus, G., Falourd, S., Hoffmann, G., Minster, B., Nouet, J., Barnola, J.M., Chappellaz, J., Fischer, H., Gallet, J.C., Johnsen, S., Leuenberger, M., Loulergue, L., Luethi, D., Oerter, H., Parrenin, F., Raisbeck, G., Raynaud, D., Schilt, A., Schwander, J., Selmo, E., Souchez, R., Spahni, R., Stauffer, B., Steffensen, J.P., Stenni, B., Stocker, T.F., Tison, J.L., Werner, M., Wolff, E.W., 2007. Orbital and Millennial Antarctic Climate Variability over the Past 800,000 Years. *Science* 317, 793-796.

Kashiwaya, K., Ryugo, M., Horii, M., Sakai, H., Nakamura, T., Kawai, T., 1999. Climato-limnological signals during the past 260,000 years in physical properties of bottom sediments from Lake Baikal. *Journal of Paleolimnology* 21, 143-150.

Kim, G.Y., Kim, D.C., 2001. Comparison and correlation of physical properties from the plain and slope sediments in the Ulleung Basin, East Sea (Sea of Japan). *Journal of Asian Earth Sciences* 19, 669-681.

Kominz, M.A., Patterson, K., Odette, D., 2011. Lithology dependence of porosity in slope and deep marine sediments. *Journal of Sedimentary Research* 81, 730-742.

Lang, N., Wolff, E.W., 2011. Interglacial and glacial variability from the last 800 ka in marine, ice and terrestrial archives. *Climate of the Past* 7, 361-380.

Laurenzi, M.A., Villa, I.M., 1987. $^{40}\text{Ar}/^{39}\text{Ar}$ chronostratigraphy of Vico ignimbrites. *Periodico di Mineralogia*, 56, 285 – 293.

[Le Bas, M.J., Le Maitre, R.W., Woolley, A.R., 1992. The construction of the total alkali-silica chemical classification of volcanic rocks. *Mineralogy and Petrology* 46, 1-22.](#)

[Leicher, N., Zanchetta, G., Sulpizio, R., Giaccio, B., Wagner, B., Nomade, S., Francke, A., Del Carlo, P., 2015. First tephrostratigraphic results of the DEEP site record from Lake Ohrid, Macedonia. *Biogeosciences Discuss.* 12, 15411-15460.](#)

- Lenz, O.K., Wilde, V., Riegel, W., 2011. Short-term fluctuations in vegetation and phytoplankton during the middle Eocene greenhouse climate; a 640-kyr record from the Messel oil shale (Germany). *International Journal of Earth Sciences*, 1851-1874.
- Lindhorst, K., Krastel, S., Reicherter, K., Stipp, M., Wagner, B., Schwenk, T., 2015. Sedimentary and tectonic evolution of Lake Ohrid (Macedonia/Albania). *Basin Research* 27, 84-101.
- Lisiecki, L.E., Raymo, M.E., 2005. A Pliocene-Pleistocene stack of 57 globally disturbed benthic $\delta^{18}\text{O}$ records. *Paleoceanography* 20, PA1003.
- Lisiecki, L.E., Raymo, M.E., 2007. Plio-Pleistocene climate evolution; trends and transitions in glacial cycle dynamics. *Quaternary Science Reviews* 26, 56-69.
- Marra, F., Karner, D.B., Freda, C., Gaeta, M., Renne, P.R. 2009. Large mafic eruptions at the Alban Hills volcanic district (Central Italy): chronostratigraphy, petrography and eruptive behaviour. *Journal of Volcanology and Geothermal Research* 179, 217–232.
- Milanković, M., 1920. *Théorie mathématique des phénomènes thermiques produits par la radiation solaire*. Gauthier-Villars et Cie, Paris.
- Molinie, A.J., Ogg, J.G., 1990a. Milankovitch cycles in Upper Jurassic and Lower Cretaceous radiolarites of the Equatorial Pacific; spectral analysis and sedimentation rate curves. *Proceedings of the Ocean Drilling Program, Scientific Results* 129, 529-547.
- Molinie, A.J., Ogg, J.G., 1990b. Sedimentation-rate curves and discontinuities from sliding-window spectral analysis of logs. *Log Analyst* 31, 370-374.
- Nomade, S., Knight, K.B., Beutel, E., Renne, P.R., Verati, C., Feraud, G., Marzoli, A., 2005. Duration and eruptive chronology of CAMP; implications for central Atlantic rifting and the Triassic-Jurassic boundary. *Eos, Transactions, American Geophysical Union* 86, @AbstractV13A-0519.
- Nowaczyk, N.R., Haltia, E.M., Ulbricht, D., Wennrich, V., Sauerbrey, M.A., Rosén, P., Vogel, H., Francke, A., Meyer-Jacob, C., Andreev, A.A., Lozhkin, A.V., 2013. Chronology of Lake El'gygytgyn sediments – a combined magnetostratigraphic, palaeoclimatic and orbital tuning study based on multi-parameter analyses. *Climate of the Past* 9, 2413-2432.
- Pälike, H., 2005. *Earth; orbital variation (including Milankovitch cycles)*. Elsevier Academic Press: Oxford, United Kingdom, pp. 410-421.

Paulissen, W.E., Luthi, S.M., 2011. High-frequency cyclicity in a Miocene sequence of the Vienna Basin established from high-resolution logs and robust chronostratigraphic tuning. *Palaeogeography, Palaeoclimatology, Palaeoecology* 307, 313-323.

Petrosino, P., Jicha, B.R., Mazzeo, F.C., Russo Ermolli, E., 2014a. A high resolution tephrochronological record of MIS 14-12 in the Southern Apennines (Acerno basin, Italy). *Journal of Volcanology and Geothermal Research* 274, 34-50.

Priestley, M.B., 1981. *Spectral analysis and time series*. New York: Academic Press.

Prokopenko, A.A., Hinnov, L.A., Williams, D.F., Kuzmin, M.I., 2006. Orbital forcing of continental climate during the Pleistocene; a complete astronomically tuned climatic record from Lake Baikal, SE Siberia. *Quaternary Science Reviews* 25, 3431-3457.

Prokopenko, A.A., Williams, D.F., Karabanov, E.B., Khursevich, G.K., 2001. Continental response to Heinrich events and Bond cycles in sedimentary record of Lake Baikal, Siberia. *Global and Planetary Change* 28, 217-226.

Rachold, V., Brumsack, H.-J., 2001. Inorganic geochemistry of Albian sediments from the Lower Saxony Basin NW Germany; palaeoenvironmental constraints and orbital cycles. *Palaeogeography, Palaeoclimatology, Palaeoecology* 174, 121-143.

Rider, M.H., Kennedy, M., 2011. *The Geological Interpretation of Well Logs*. Rider-French Consulting Limited, 3rd edition: Glasgow, Scotland.

Rotolo, S.G., Scaillet, S., La Felice, S., Vita-Scaillet, G., 2013. A revision of the structure and stratigraphy of pre-Green Tuff ingimbrites at Pantelleria (Strait of Sicily). *Journal of Volcanology and Geothermal Research*, 250, 61-74.

Scholz, C.A., Talbot, M.R., Brown, E.T., Lyons, R.P., 2011. Lithostratigraphy, physical properties and organic matter variability in Lake Malawi drillcore sediments over the past 145,000 years. *Palaeogeography, Palaeoclimatology, Palaeoecology* 303, 38-50.

Serra, O., Serra, L., 2003. *Well Logging and Geology*. Serralog 2003, France.

Steiger, R.H., Jäger, E., 1977. Subcommission on geochronology: Convention on the use of decay constants in geo- and cosmochronology. *Earth and Planetary Science Letters* 36, 359-362.

~~Stockhecke, M., Sturm, M., Brunner, I., Schmineke, H.-U., Sumita, M., Kipfer, R., Cukur, D., Kwiecien, O., Anselmetti, F.S., 2014. Sedimentary evolution and environmental history of Lake Van (Turkey) over the past 600 000 years. *Sedimentology* 61, 1830-1861.~~Stockhecke,

[M., Kwiecien, O., Vigliotti, L., Anselmetti, F.S., Beer, J., Çağatay, M.N., Channell, J.E.T., Kipfer, R., Lachner, J., Litt, T., Pickarski, N., Sturm, M., 2014. Chronostratigraphy of the 600,000 year old continental record of Lake Van \(Turkey\). Quaternary Science Reviews 104, 8-17.](#)

Sulpizio, R., Zanchetta, G., D'Orazio, M., Vogel, H., Wagner, B., 2010. Tephrostratigraphy and tephrochronology of lakes Ohrid and Prespa, Balkans. *Biogeosciences* 7, 3273-3288.

Theys, P.P., 1991. Log data acquisition and quality control. Editions Technip: Paris, France.

Torrence, C., Compo, G.P., 1998. A Practical Guide to Wavelet Analysis. *Bulletin of the American Meteorological Society* 79, 61-78.

Trajanovski, S., Albrecht, C., Schreiber, K., Schultheiß, R., Stadler, T., Benke, M., Wilke, T., 2010. Testing the spatial and temporal framework of speciation in an ancient lake species flock: The leech genus *Dina* (Hirudinea: Erpobdellidae) in Lake Ohrid. *Biogeosciences* 7, 3387-3402.

Vogel, H., Wagner, B., Zanchetta, G., Sulpizio, R., Rosen, P., 2010a. A paleoclimate record with tephrochronological age control for the last glacial-interglacial cycle from Lake Ohrid, Albania and Macedonia. *Journal of Paleolimnology* 44, 295-310.

Vogel, H., Wessels, M., Albrecht, C., Stich, H.-B., Wagner, B., 2010b. Spatial variability of recent sedimentation in Lake Ohrid (Albania/Macedonia). *Biogeosciences* 7, 3333-3342.

Vogel, H., Zanchetta, G., Sulpizio, R., Wagner, B., Nowaczyk, N., 2010c. A tephrostratigraphic record for the last glacial-interglacial cycle from Lake Ohrid, Albania and Macedonia. *Journal of Quaternary Science* 25, 320-338.

Wagner, B., Reicherter, K., Daut, G., Wessels, M., Matzinger, A., Schwalb, A., Spirkovski, Z., Sanxhaku, M., 2008. The potential of Lake Ohrid for long-term palaeoenvironmental reconstructions. *Palaeogeography, Palaeoclimatology, Palaeoecology* 259, 341-356.

Wagner, B., Wilke, T., Grazhdani, A., Kostoski, G., Krastel, S., Reicherter, K.R., Zanchetta, G., 2009. SCOPSCO; Scientific Collaboration On Past Speciation Conditions in Lake Ohrid. *Eos, Transactions, American Geophysical Union* 90, @AbstractPP14A-02.

Wagner, B., Wilke, T., Krastel, S., Zanchetta, G., Sulpizio, R., Reicherter, K., Leng, M., Grazhdani, A., Trajanovski, S., Levkov, Z., Reed, J., Wonik, T., 2014. More Than One Million Years of History in Lake Ohrid Cores. *EOS, Transactions, American Geophysical Union* 95, 25-32.

Weedon, G., 2003. Time-series analysis and cyclostratigraphy; examining stratigraphic records of environmental cycles. Cambridge University Press: Cambridge, United Kingdom.

Wonik, T., 2001. Gamma-ray measurements in the Kirchrode I and II boreholes. *Palaeogeography, Palaeoclimatology, Palaeoecology* 174, 97-105.

Wu, H., Zhang, S., Feng, Q., Jiang, G., Li, H., Yang, T., 2012. Milankovitch and sub-Milankovitch cycles of the early Triassic Daye Formation, South China and their geochronological and paleoclimatic implications. *Gondwana Research* 22, 748-759.

Table 1

	(LR04)	(tephra		
depth	<u>age from</u> <u>points</u>	<u>age from</u> <u>pointser</u>	<u>tie</u> correlated eruption/tephra	reference
mblf	ka	ka		
1.46	4			
13.67		29	Y-3	Albert et al., 2014
19.35		39	Y-5 (Campanian Ignimbrite)	De Vivo et al., 2001
24.37	49			
30.17	62			
36.41	78			
40.10	87			
48.40		109 +/- 2	X-6	Iorio et al., 2013
55.11		129 +/- 6	P11	Rotolo et al., 2013
59.19	140			
66.73		162 +/- 6	Vico B	Laurenzi and Villa, 1987
74.61	171			
85.09	185			
97.00	206			
103.40	223			
106.48	230			
112.10	246			
121.75	271			
132.92	294			
144.00	317			
150.65	342			

153.76	350			
161.52	374			
167.80	392			
170.04	398			
178.29	433			
183.28	456	457 +/- 2	Pozzolane Rosse	Giaccio et al., 2013
201.31	508			
203.05		511 +/- 6	Acerno A10-A9	Petrosino et al., 2014
206.70		527 +/- 2	Tufo Bagni Albule	Marra et al., 2009
209.09	536			
212.89	549			
215.53	557			
219.20	568			
220.99	574			
225.44	585			
240.00	630			

Figure captions

Fig. 1-a) Regional map of Lake Ohrid in the Mediterranean region and (b) bathymetric map of the lake. The city of Ohrid and the DEEP drill site from the ICDP campaign are shown (modified after Wagner et al., 2014).

~~Regional and bathymetric map of Lake Ohrid (modified after Wagner et al., 2014). The city of Ohrid and the DEEP drill sites from the ICDP campaign in spring 2013 are shown.~~

Fig. 2-a) Correlation of downhole GR and K data from 0 to 240 mblf with LR04 (Lisiecki and Raymo, 2005) from 0 to 630 ka. The age-depth ~~age-range~~ was set by eight anchor points from tephrochronology. Warm and / or humid periods correlate with periods of low GR and K values. K – potassium content from spectral gamma ray, GR – total gamma radiation, MIS – Marine Isotope Stages, mblf – metres below lake floor.

Fig. 2-b) An age scale was applied to the downhole logging data (GR and K) based on tie points to LR04 (Lisiecki and Raymo, 2005) and ~~age-marker points~~ from tephrochronology. K – potassium content from spectral gamma ray, GR – total gamma radiation, MIS – Marine Isotope Stages, mblf – metres below lake floor.

Fig. 2-c) A synthetic curve calculated by ~~simple~~ linear regression between GR on age-time scale and LR04. Both curves are displayed as overlay ~~and~~ three zones are identified. A) 630 to 430 ka (MIS 15 to 12), B) 430 to 185 ka (MIS 11 to 7) and, C) 185 to 0 ka (MIS 6 to 1). $\delta^{18}\text{O}_{\text{calc}}$ is prevailing decreased during zones ~~1A)~~ and ~~3C)~~ (dark green colour) and higher in zone ~~2B)~~ (light green colour) compared to LR04. MIS - Marine Isotope Stages.

Fig. 3-a) Three-dimensional spectrogram from sliding window analysis of GR data from 0 to 240 mblf. The relative power of the frequency components is indicated by colour and two spectral peaks with wavelengths of 30 m and 45 m are apparent. Based on the break in the spectral characteristics at about 110 mblf, the spectral plot was subdivided into a lower interval I (240 to 110 mblf) and an upper interval II (110 to 0 mblf). ~~Two-s~~Single spectrum spectra of GR ~~within-from~~ interval I at 170 mblf (~~leftb~~) and ~~from~~ interval II at 50 mblf (~~rightc~~) are displayed below ~~and show that T~~the ~~emphasized~~ wavelengths of 30-m for interval I and ~~and~~ 45 m for interval II are prominent ~~in the single spectra.~~ The dashed line separates the spectral background from the spectral peaks.

Fig. 4 Estimates of sedimentation rates from 0 to 240 mblf based on visual correlation and tying to the timescale of LR04 (blue; Lisiecki and Raymo, 2005) and sliding window analysis and-with linking of high amplitudes to the 100 ka cycle (green). The sedimentation rates from sliding window analysis show an increase from 30 ~~em/ka~~ to 45 ~~em/ka~~cm/kyr at about 110 mblf, whereas results from tie points are more variable and range from 22 to 71 ~~em/ka~~cm/kyr. The dashed red line indicates the mean values of the sedimentation rates from LR04 tie points for interval I and II. MIS stages from ~~MIS-1~~ to 15 are ~~indicated~~labelled. MIS – Marine Isotope Stages, mblf – metres below lake floor.

Fig. 5a): Porosity values derived from sonic (V_p) after Erickson and Jarrard (1998) from 30 to 250 mblf. Average values for intervals of 100 m length were calculated as indicated by the black line and values for the top 30 m of the sediments were linear interpolated (dashed black line). An ~~The~~ initial porosity (surface porosity) of 80% was used for modelling of compaction by 2D Move. Φ – porosity, V_p – p-wave velocity from sonic, mblf – metres below lake floor.

Fig. 5b) Sediment layers of thicknesses of 50 m are modelled ~~by use of~~applying the software 2D Move. ~~From a~~The cumulative present layer thickness of 250 m, ~~the original thickness is extended~~ after decompaction ~~of the sediment column was estimated at to~~ 285 m (original layer thickness).

Fig. 5c) The GR data from 0 to 240 mblf and the intervals from subdivision by spectral characteristics at about 110 mblf (left). The data was stretched to the estimates of the original layer thicknesses. The decompacted depth of the sediment layers and the resulting increased lengths of GR and new interval borders are displayed (right).

Fig. 5d): Result from sliding window analysis of ~~stretched~~ GR data on decompacted depth scale. Two spectral peaks with wavelengths of 36 ~~m~~ and 48 m are emphasized. GR – gamma ray, mblf – metres below lake floor.

Fig. 6: Age-Depth-depth age model for the sediment depths of 0 to 240 mblf. The two ~~curves~~ sedimentation rates were generated by visual tying to LR04 (blue line; Lisiecki and Raymo, 2005) and by linking of prominent cycles to the 100 ~~ka~~kyr signal (green line). Tephra tie points are indicated by red triangles. mblf – metres below lake floor.

Table caption

Tab. 1: ~~The d~~Downhole logging data correlated to LR04 (Lisiecki and Raymo, 2005). Eight anchor points from tephrochronology and 30 additional tie points of significant features between the downhole data and LR04 are set. The tephra ages were recalculated (except Y-3) according relative to ACs-2 at 1.193 Ma (Nomade et al., 2005) and the total decay constant of Steiger and Jäger (1977), uncertainties are 2δ . mblf – metres below lake floor.

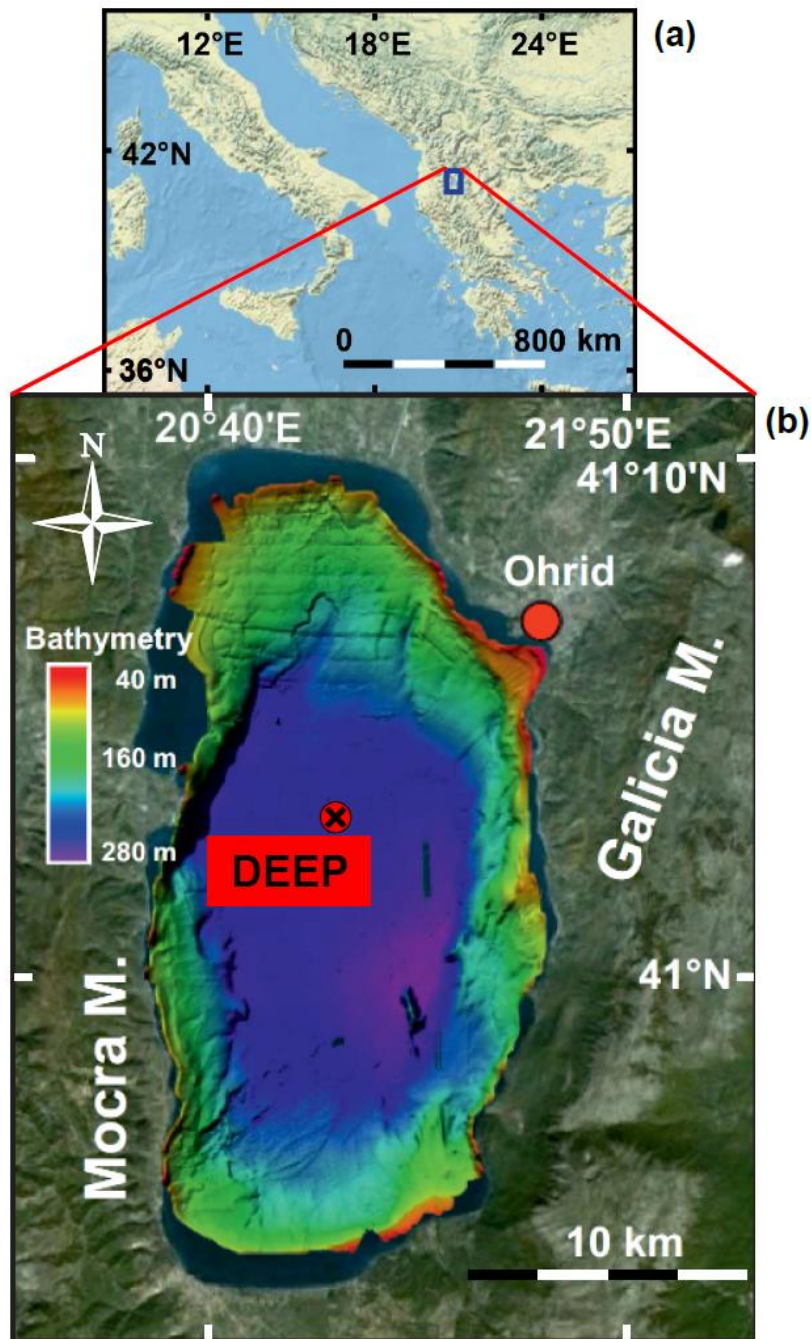


Fig. 1a, b

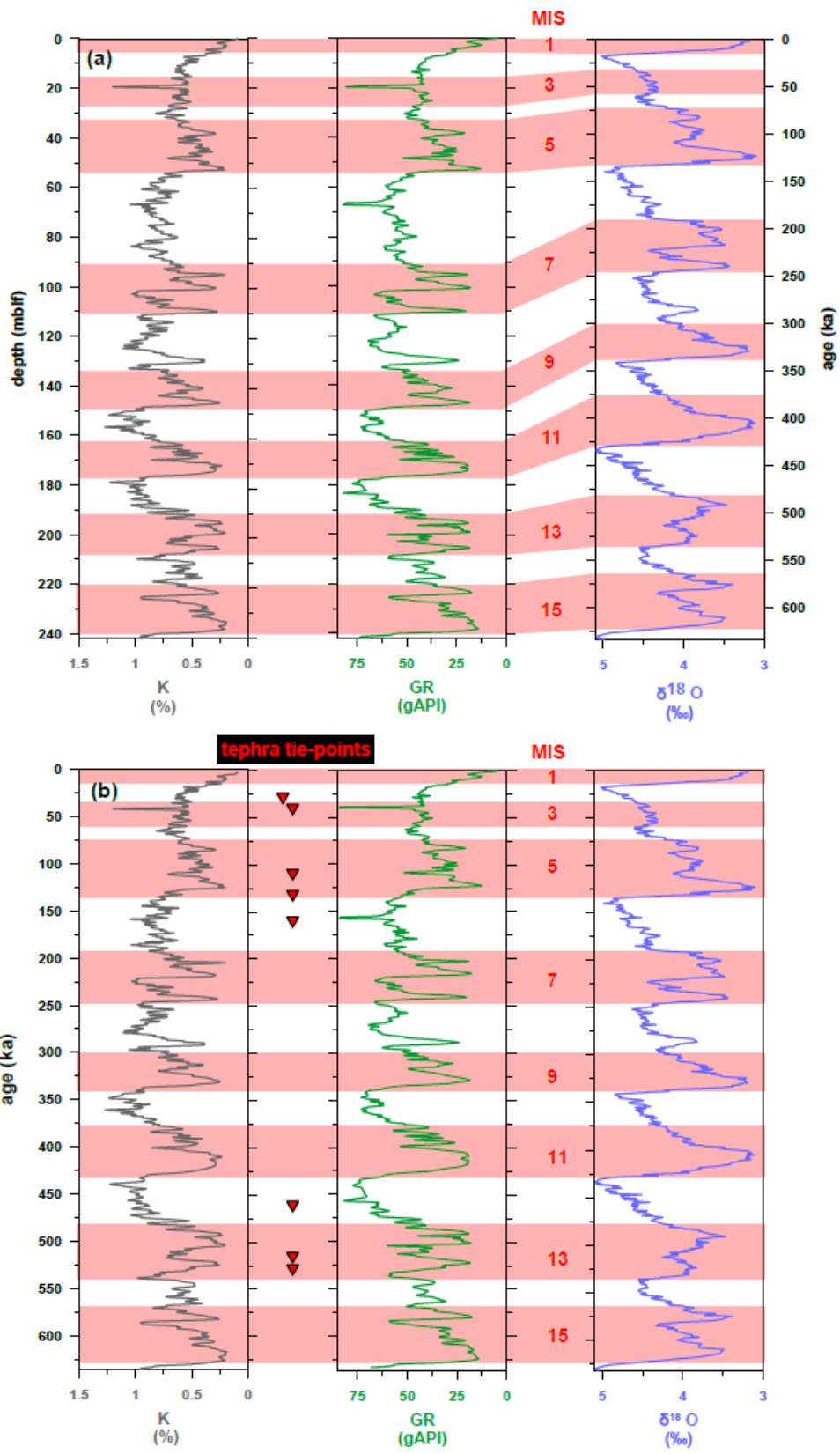


Fig. 2a, b

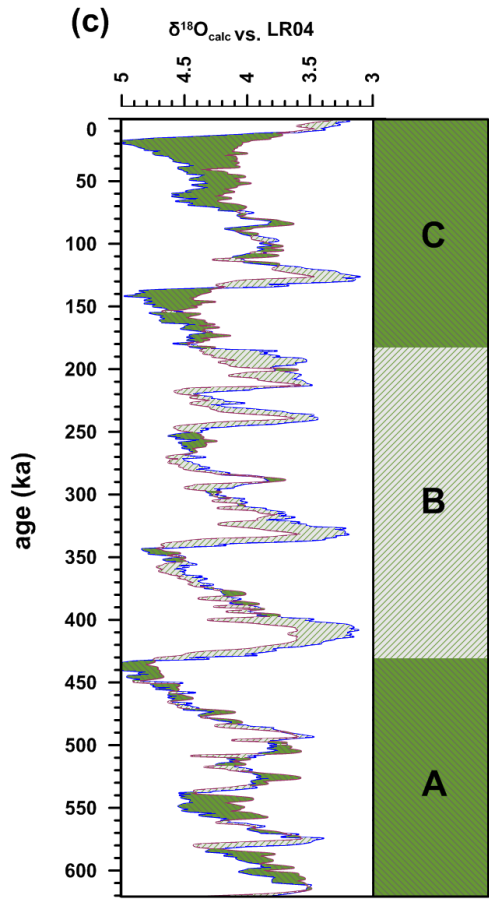


Fig. 2c

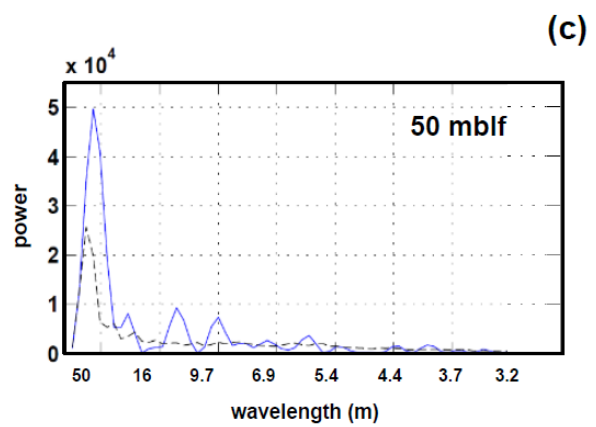
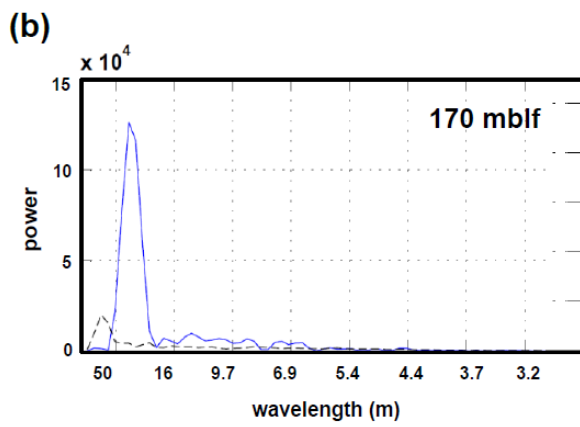
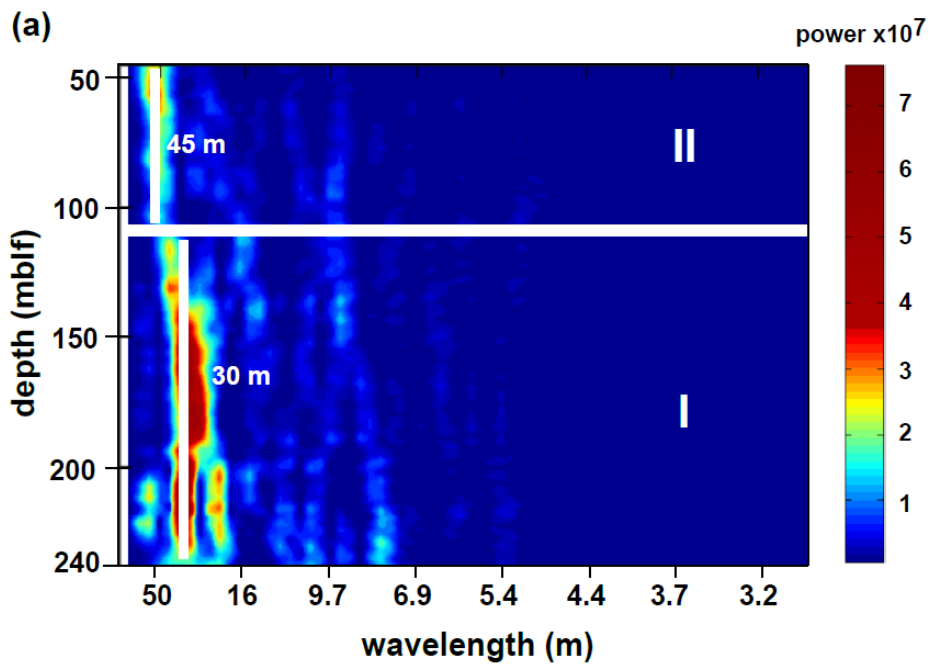


Fig. 3a, b, c

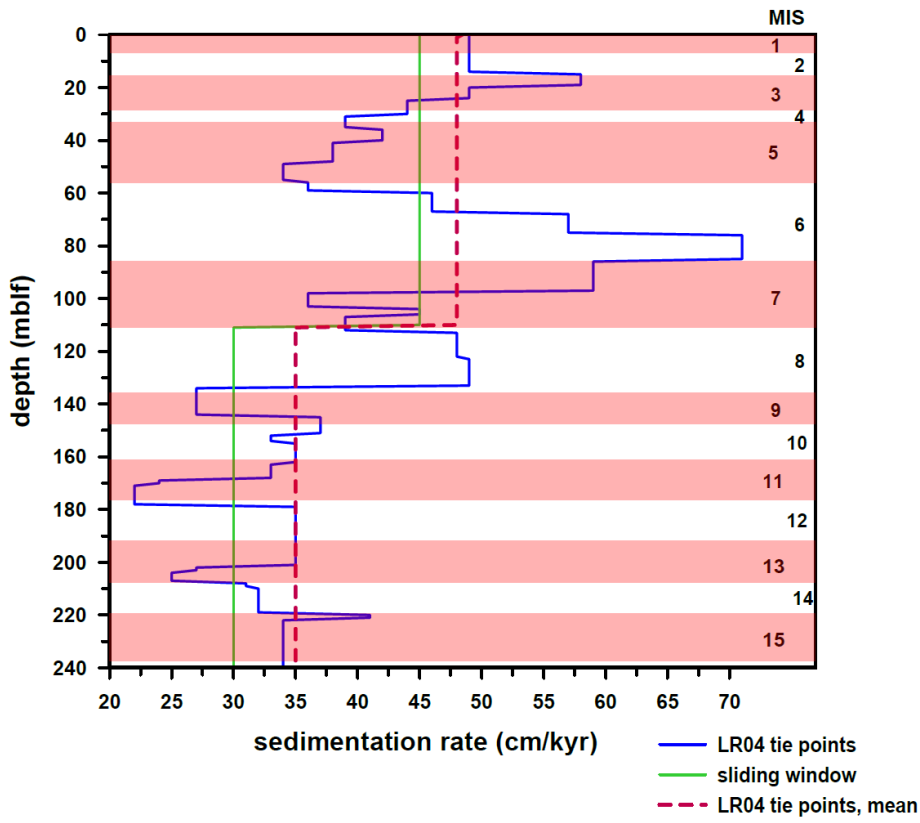


Fig. 4

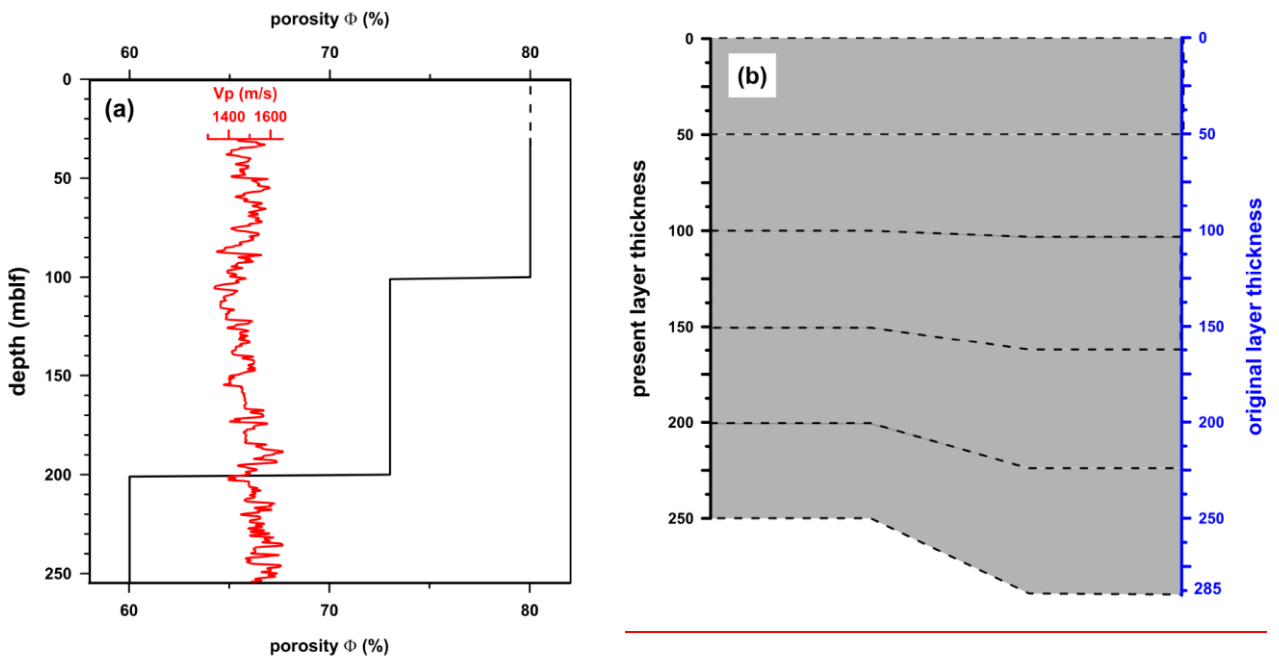


Fig. 5a, b

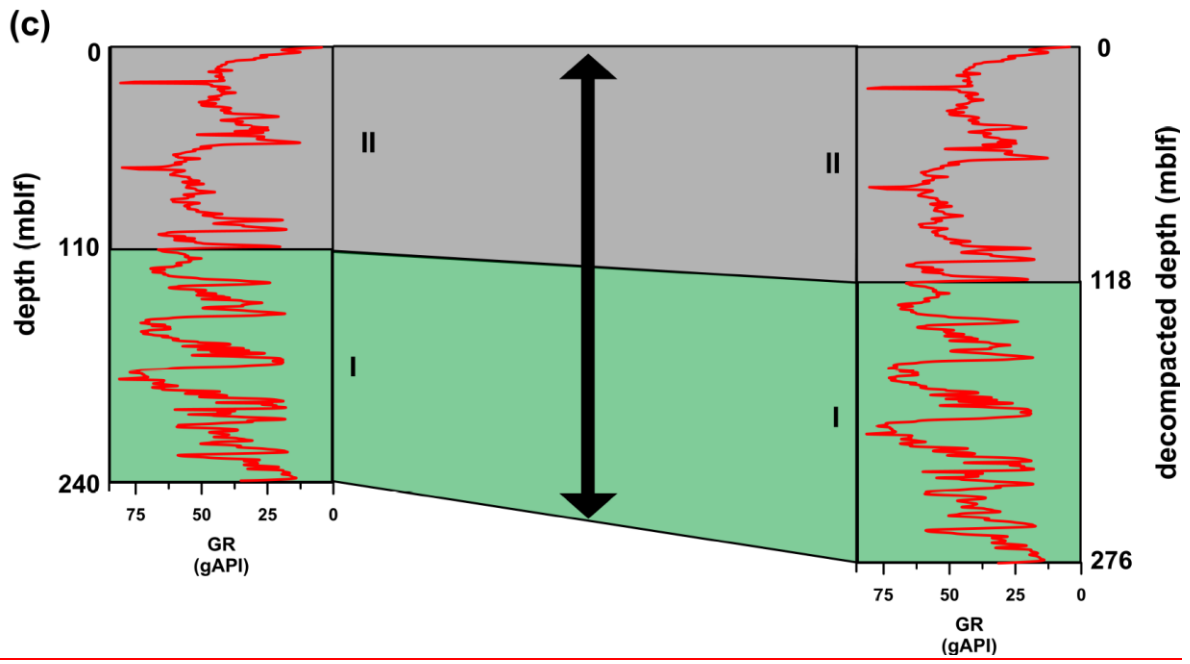


Fig. 5c

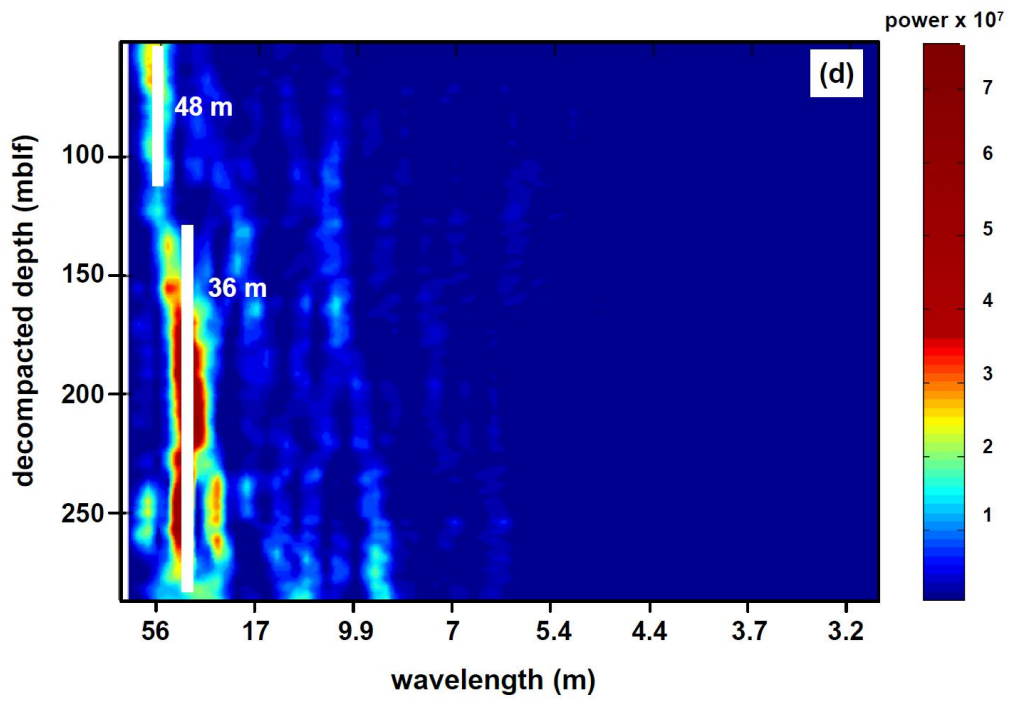


Fig. 5d

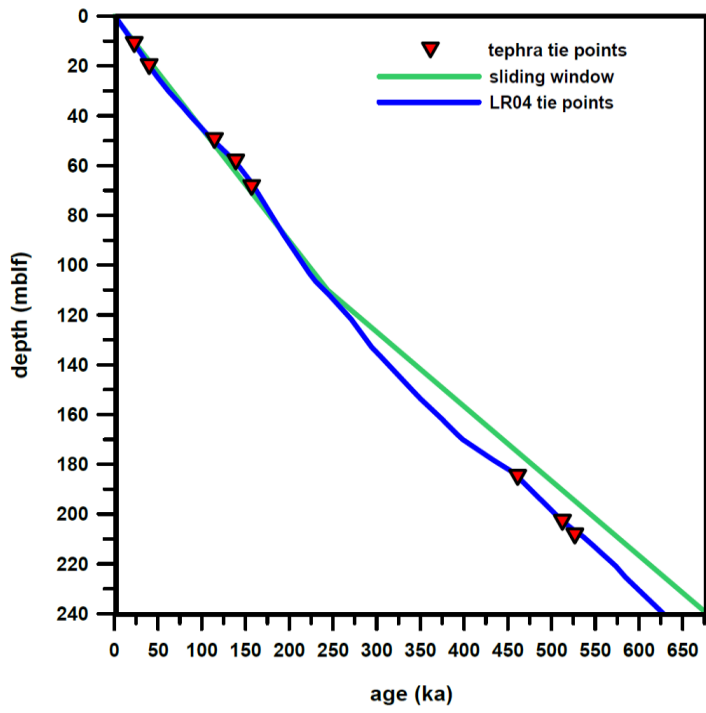


Fig. 6